

Double Gamow-Teller transitions and its relation to neutrinoless $\beta\beta$ decay

Noritaka Shimizu,^{*} Javier Menéndez,[†] and Kentaro Yako

Center for Nuclear Study, The University of Tokyo, Bunkyo-ku, Hongo, Tokyo 113-0033, Japan

(Dated: March 13, 2022)

We study the double Gamow-Teller (DGT) strength distribution of ^{48}Ca with state-of-the-art large-scale nuclear shell model calculations. Our analysis shows that the centroid energy of the DGT giant resonance depends mostly on the isovector pairing interaction, while the resonance width is more sensitive to isoscalar pairing. Pairing correlations are also key in neutrinoless $\beta\beta$ ($0\nu\beta\beta$) decay. We find a simple relation between the centroid energy of the ^{48}Ca DGT giant resonance and the $0\nu\beta\beta$ decay nuclear matrix element. More generally, we observe a very good linear correlation between the DGT transition to the ground state of the final nucleus and the $0\nu\beta\beta$ decay matrix element. The correlation, which originates on the dominant short-range character of both transitions, extends to heavier systems including several $\beta\beta$ emitters, and also holds in energy-density functional results. Our findings suggest that DGT experiments can be a very valuable tool to obtain information on the value of $0\nu\beta\beta$ decay nuclear matrix elements.

PACS numbers: 24.30Cz, 23.40.-s, 23.40Hc, 21.60.Cs

Keywords: Double Gamow-Teller giant resonance, Neutrinoless double-beta decay, Nuclear shell model

Introduction. The quest for the detection of neutrinoless $\beta\beta$ ($0\nu\beta\beta$) decay is one of major experimental challenges in particle and nuclear physics [1–4]. $0\nu\beta\beta$ decay is the most promising process to observe lepton-number violation in the laboratory. Its discovery would prove that neutrinos are its own antiparticles (Majorana particles), provide information on the absolute neutrino mass, and give insight on the matter-antimatter asymmetry of the universe [5]. The $0\nu\beta\beta$ decay lifetime depends on the nuclear matrix element (NME), which has to be calculated and is sensitive to the nuclear structure of the parent and daughter nuclei. Nuclear many-body approaches disagree in their prediction of NMEs by more than a factor two. Furthermore these results may need an additional renormalization, or “quenching”, of a similar amount [6]. This theoretical uncertainty limits severely the capability to anticipate the reach of future $0\nu\beta\beta$ decay experiments, and the extraction of the neutrino mass once a decay signal has been observed.

Given the difficulty of theoretical calculations to agree on the value of the $0\nu\beta\beta$ decay NMEs, experimental data on the nuclear structure of the parent and daughter nuclei [7–10], two-nucleon transfer reactions [11], or the lepton-number-conserving two-neutrino $\beta\beta$ decay [12–17] have been proposed to test the many-body approaches and shed light on the NME values. Charge-exchange reactions, where a proton is replaced by a neutron or the other way around, provide information on the Gamow-Teller (GT) strengths [18–20], offering another good test of the theoretical calculations [21–23]. The GT strength of the parent to intermediate nuclei, combined with the strength of the daughter to intermediate nuclei, is related to two-neutrino $\beta\beta$ decay. However the connection is not straightforward because the relative phase between the two GT contributions cannot be measured. Despite all these efforts an observable clearly correlated to $0\nu\beta\beta$ decay remains to be found.

Double charge-exchange reactions have been suggested to resemble $0\nu\beta\beta$ decay [24, 25]. The detection of the resulting new collective motion is, however, challenging. While the double isobaric analogue resonance was found via pion double charge-exchange reactions [26], the double Gamow-Teller giant resonance (DGT GR) remains to be observed three decades after the first detailed theoretical predictions [27–31]. A more recent study was carried out in Ref. [32]. Modern searches of the DGT GR are based on novel heavy-ion double charge-exchange reactions [33, 34]. The data analysis of experiments performed at RNCP Osaka are recent [34] or ongoing [35], and a similar experiment is planned at RIBF RIKEN [36]. Double charge-exchange reactions will be used at LNS Catania aiming to give insight on $0\nu\beta\beta$ decay NMEs [25].

Present DGT GR searches use the lightest $\beta\beta$ emitter ^{48}Ca as target. Several experimental [37–39] and theoretical works [14, 40–46] have investigated the $0\nu\beta\beta$ decay of this nucleus. In this Letter we analyze the ^{48}Ca DGT strength distribution in connection to $0\nu\beta\beta$ decay. We focus on the correlation between the properties of the DGT GR and the $0\nu\beta\beta$ decay NME. In addition we study the relation between the DGT transition to the ground state of the final nucleus and the NME, exploring the extension to heavier $\beta\beta$ decay emitters.

Double Gamow-Teller transitions. The DGT transition probability, or strength, is defined as

$$B(\text{DGT}^\pm; \lambda; i \rightarrow f) = \frac{1}{2J_i + 1} |\langle f || \mathcal{O}_\pm^{(\lambda)} || i \rangle|^2, \quad (1)$$

with J_i the total angular momentum of the initial (i) nucleus. The DGT operator couples two GT ones $\mathcal{O}_\pm^{(\lambda)} = [\sum_j \sigma_j \tau_j^\pm \times \sum_j \sigma_j \tau_j^\pm]^{(\lambda)}$, where σ is the spin, τ^- (τ^+) makes a neutron a proton (vice versa) and j sums over all nucleons. The DGT operator can have rank $\lambda = 0, 2$, due to symmetry. For ^{48}Ca $J_i^\pi = 0^+$ and the DGT strength populates $J_f^\pi = 0^+, 2^+$ states of the final (f) ^{48}Ti .

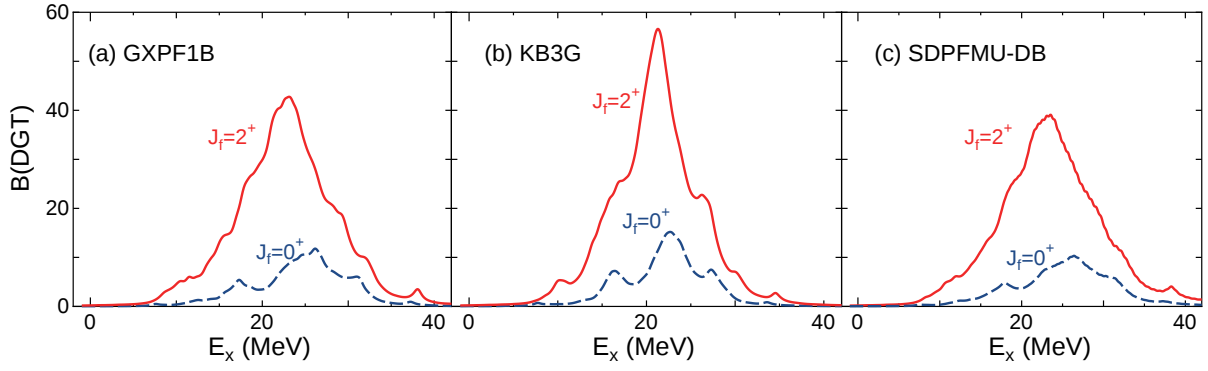


FIG. 1. DGT strength distribution of ^{48}Ca to ^{48}Ti . The red solid (blue dashed) line shows the $B(\text{DGT}^-; \lambda = 2)$ [$B(\text{DGT}^-; \lambda = 0)$] transitions. Results obtained with the (a) GXPF1B [50], (b) KB3G [51] nuclear interactions in the single pf shell, and (c) SDPFMU-DB [41] interaction (an extension of GXPF1B) in the two-shell sd - pf configuration space.

We perform large-scale shell-model calculations to study the DGT strength distribution of ^{48}Ca with the Lanczos strength function method [47, 48]. This technique is based on acting with the DGT operator on the initial state of the transition, the ^{48}Ca ground state. After typically 300 iterations, the states obtained are still not exact eigenstates of the nuclear interaction but the strength distribution is a very good approximation to the exact one [48]. When necessary we project into good angular-momentum diagonalizing the J^2 operator. The DGT calculations use the M -scheme shell-model code KSHELL [49]. We smear out the final DGT distributions with Lorentzians of $\Gamma = 1$ MeV width to simulate the experimental energy resolution.

Figure 1 (a) and (b) shows the DGT strength distribution obtained with two different nuclear interactions [50, 51] in the configuration space comprised by one harmonic oscillator major shell (pf shell). The results in Fig. 1 (c) use an interaction acting in two major shells [41] (sd and pf shells), limited to $2\hbar\omega$ excitations. The three DGT distributions are in reasonable agreement, suggesting that the theoretical uncertainties due to the nuclear interaction and the size of the configuration space are relatively under control. For instance, the DGT GR centroid energy only differs by 1.6 MeV between the two one-major-shell calculations.

DGT GR, pairing and $0\nu\beta\beta$ decay. Next we analyze the properties of the DGT strength distribution. We probe its dependence on pairing correlations by adding to the nuclear interaction

$$H' = H + G^{JT} P^{JT}, \quad (2)$$

where $P^{J=0,T=1}$ and $P^{J=1,T=0}$ denote the isovector and isoscalar pairing interactions [52], respectively, with corresponding G^{01} and G^{10} couplings. For H we take the pf -shell GXPF1B interaction, but alternatively using KB3G gives similar results.

Figure 2 (a) shows the DGT strength distribution for various values, attractive and repulsive, of the ad-

ditional isovector pairing term. The top panel shows the $G^{01} = 0.5$ MeV case, where most of the isovector pairing of the original interaction is canceled [53], while the bottom panel uses $G^{01} = -0.5$ MeV, greatly enhancing isovector pairing correlations. The centroid energy of the DGT distribution, both for $\lambda = 0$ and $\lambda = 2$ couplings, increases with the strength of the isovector pairing interaction, while the DGT GR width remains rather stable. Likewise Fig. 2 (b) shows the DGT strength distribution for isoscalar pairing couplings G^{10} ranging from repulsive values that almost cancel this interaction [53] to attractive ones. The centroid energy of the DGT GR is rather independent of the isoscalar pairing coupling. In contrast, strongly attractive isoscalar pairing makes the DGT GR width broader than with the original nuclear interaction.

The $0\nu\beta\beta$ decay NMEs are also very sensitive to pairing correlations, both isovector [54–56] and isoscalar [57–60]. The $0\nu\beta\beta$ decay NME is given by a combination of GT, Fermi (F) and tensor (T) components [6]:

$$M^{0\nu} = M_{GT}^{0\nu} - \left(\frac{g_V}{g_A}\right)^2 M_F^{0\nu} + M_T^{0\nu}, \quad (3)$$

$$M_X^{0\nu} = \langle f | \sum_{jk} \tau_j^- \tau_k^- S_X V_X(r_{jk}) | i \rangle, \quad (4)$$

where $g_A/g_V = 1.27$ is the ratio of the axial and vector couplings, the different spin structures are $S_F = 1$, $S_{GT} = \sigma_j \sigma_k$ and the tensor S_T , and V_{GT} , V_F and V_T are the corresponding neutrino potentials, which depend on the distance between the decaying neutrons r_{jk} . Equation (3) uses the closure approximation, which is accurate to more than 90% [44]. In this approximation the neutrino potential is the only difference between the dominant term $M_{GT}^{0\nu}$ and the DGT operator.

We combine the sensitivity to pairing correlations of the DGT strength distribution, and the well-known sensitivity of the $0\nu\beta\beta$ decay NME to these correlations, by studying both observables with H' obtained with various

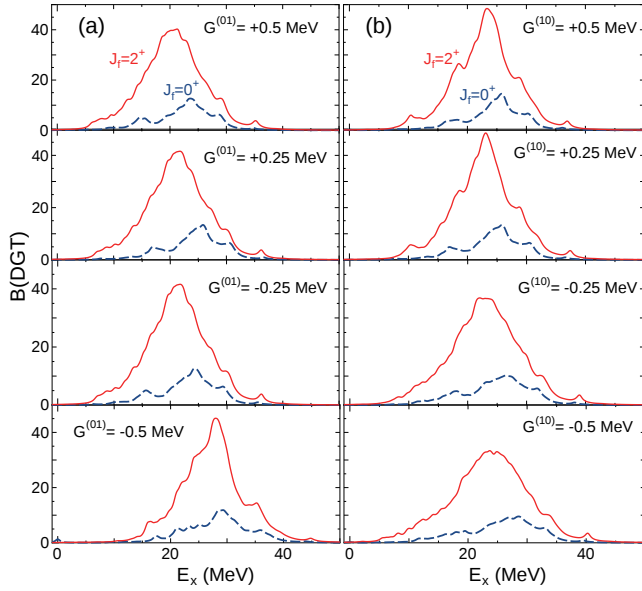


FIG. 2. DGT strength distribution for a range of values from 0.5 MeV (top panels) to -0.5 MeV (bottom) of the couplings added to the GXPF1B interaction: (a) $G^{(01)}$ of the isovector pairing term, (b) $G^{(10)}$ of the isoscalar pairing term. Solid red (dashed blue) lines show $\lambda = 2$ ($\lambda = 0$) DGT distributions.

coupling values. Figure 3 shows NMEs as a function of the centroid energy of the DGT distribution, defined as

$$E_c = \frac{\sum_f E_f B(DGT^-, i \rightarrow f)}{\sum_f B(DGT^-, i \rightarrow f)}. \quad (5)$$

Figure 3 highlights that the NME, dominated by $M_{GT}^{0\nu}$, is well correlated with the average energy of the DGT GR. This correlation, driven by the dependence of both observables to the isovector pairing strength, agrees well with the results obtained in two major shells, indicated by an open circle in Fig. 3. This consistency supports the use of the modified interaction H' , which may capture sufficiently well the aspects relevant for the DGT GR – $0\nu\beta\beta$ decay correlation without the need to reproduce all other nuclear structure properties. Our study indicates that a measurement of the DGT GR, besides testing the theoretical calculation, can provide a hint of the NME value. A measured centroid energy above (below) the result of the original nuclear interaction would suggest a larger (smaller) NME than the initial GXPF1B prediction. Figure 3 indicates that an experimental uncertainty on the DGT GR peak of a couple of MeV, which might be experimentally accessible in the near future [25, 35, 36], would be sufficient to shed light on the ^{48}Ca $0\nu\beta\beta$ decay NME. On the other hand, while we find that a narrower DGT GR is associated with a larger NME, very small uncertainties below the MeV scale would be needed to extract information relevant for $0\nu\beta\beta$ decay.

The correlation in Fig. 3 is useful if the shell model can reproduce the DGT GR. This will be tested once DGT

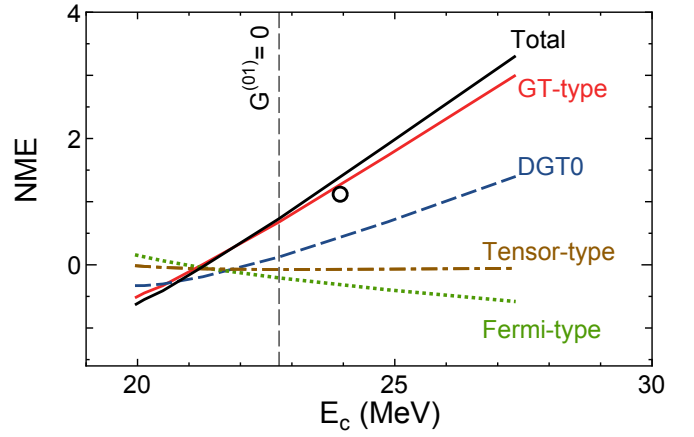


FIG. 3. $0\nu\beta\beta$ decay NME and DGT GR ($\lambda = 2$) centroid energy (E_c), for the interactions defined in Eq. (2). The black solid, red solid, green dotted and brown dashed-dotted lines show the total, GT, Fermi and tensor NME parts, respectively. The blue dashed line denotes the DGT transition to the ^{48}Ti ground state. The vertical dashed line indicates the results of the original GXPF1B interaction. The open circle corresponds to the two-shell total result in the sd - pf space.

data is available. For the moment, shell model predictions for the GT strength distribution of ^{48}Ca [61, 62], including the GT GR, agree quite well with experiment.

DGT and $0\nu\beta\beta$ decay NME. Figure 1 shows that the DGT transition into the ground state (gs) of ^{48}Ti is a tiny fraction of the total DGT distribution. Nonetheless this matrix element is expected to be the closest to $0\nu\beta\beta$ decay since both processes share initial and final states. We define the DGT matrix element as

$$M^{\text{DGT}} = \sqrt{B(DGT^-, 0; 0_{\text{gs},i}^+ \rightarrow 0_{\text{gs},f}^+)} \\ = \left| \langle 0_{\text{gs},f}^+ | \left[\sum_{j,k} [\sigma_j \tau_j^- \times \sigma_k \tau_k^-]^0 \right] | 0_{\text{gs},i}^+ \rangle \right|. \quad (6)$$

The DGT matrix element is proportional to the two-neutrino $\beta\beta$ decay matrix element evaluated in the closure approximation. The ^{48}Ca M^{DGT} shown in Fig. 3 is indeed correlated to the $0\nu\beta\beta$ decay NME.

Figure 4 explores the relation between $M^{0\nu}$ and M^{DGT} matrix elements for twenty-six pairs of initial and final nuclei comprising initial calcium, titanium and chromium isotopes with mass numbers $42 \leq A \leq 60$ (panel a); and seventeen initial germanium, selenium, tin, tellurium and xenon isotopes with masses $76 \leq A \leq 136$ that include five $\beta\beta$ emitters (panel b). We have used various one-major-shell nuclear interactions [46, 63–65] in each mass region. These interactions have been tested in nuclear spectroscopic studies and reproduce experimental two-neutrino $\beta\beta$ decay matrix elements and GT strengths to low-lying states with a renormalization of the $\sigma\tau$ operator [22, 66–68]. Figure 4 shows a simple linear relation between the DGT and $0\nu\beta\beta$ decay matrix elements, valid

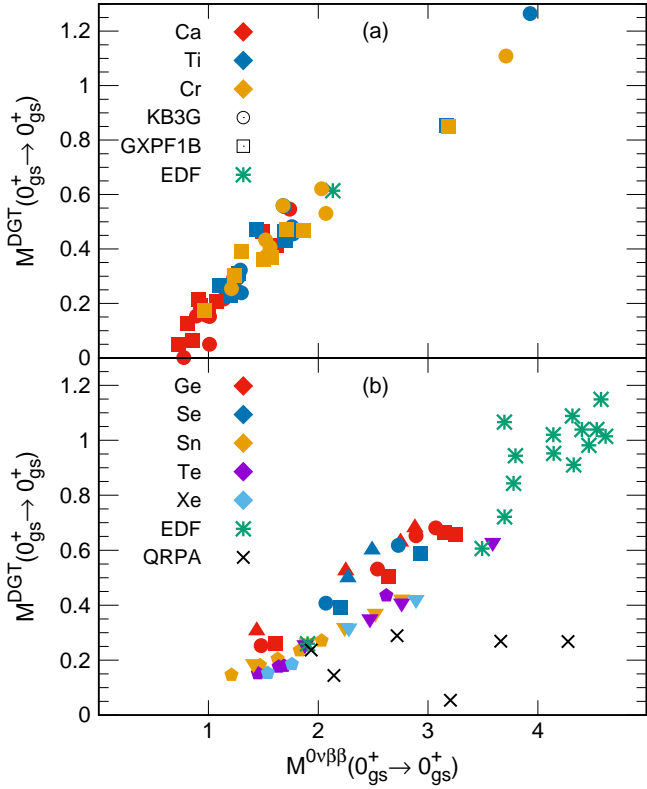


FIG. 4. Correlation between the $0\nu\beta\beta$ decay NME $M^{0\nu}$ and the DGT matrix element M^{DGT} . (a) Calcium (red), titanium (blue) and chromium (yellow) isotopes calculated with the shell model GXPF1B (squares) and KB3G (circles) interactions, compared to the EDF ^{48}Ca result [24] (green star). (b) Germanium (red), selenium (blue), tin (orange), tellurium (purple) and xenon (light blue) shell model results (filled symbols) calculated with the interactions in Refs. [46, 63–65], each one represented by a different symbol. Compared are EDF [24] (green stars) and QRPA [69] (black crosses) results for $\beta\beta$ emitters, and cadmium EDF values.

up to $M^{0\nu} \simeq 5$. When taking nuclear states truncated in the seniority basis (using the code NATHAN [48]) the same linear relation extends to $M^{0\nu} \simeq 10$. The correlation is also common to calculations in one or two major shells for results in Fig. 4 (a).

Furthermore, Fig. 4 compares the shell model results with the nonrelativistic energy-density functional (EDF) ones for $\beta\beta$ decay emitters and cadmium isotopes from Ref. [24]. The two many-body approaches follow a quite similar correlation. This is very encouraging given the marked differences between the shell model and EDF $M^{0\nu}$ values [70]. On the contrary, the quasiparticle random-phase approximation (QRPA) calculations for $\beta\beta$ decay emitters from Ref. [69] give small $M^{\text{DGT}} \lesssim 0.4$ matrix elements independently of the associated $0\nu\beta\beta$ decay NME values.

In order to understand the connection between the two processes, Fig. 5 (a) shows the matrix element distribu-

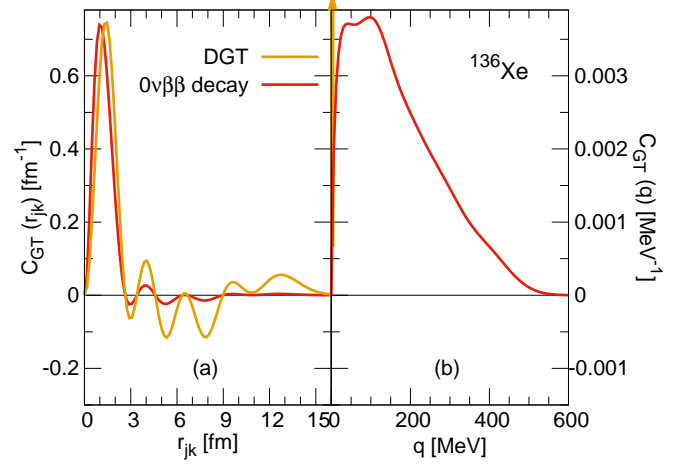


FIG. 5. Normalized distributions C_{GT} of the $M_{GT}^{0\nu}$ (red) and M^{DGT} (orange) matrix elements of ^{136}Xe as a function of (a) the internucleon distance r_{jk} , (b) the momentum transfer q . Results obtained with the nuclear interaction from Ref. [46].

tions as a function of the distance between the transferred or decaying nucleons [71]. ^{136}Xe is chosen as an example. Both matrix elements are dominated by short internucleon distances. In the case of DGT transitions this is because the intermediate- and long-range contributions cancel to a good extent. Radial distributions in the other DGT matrix elements we have studied can be somewhat different, but the approximate cancellation between intermediate and long internucleon distances is systematically observed. By contrast, Fig. 5 (b) shows that the momentum transfers are quite different, vanishing for DGT transitions and peaking around 100 MeV in $0\nu\beta\beta$ decay.

The short range character of both DGT and $0\nu\beta\beta$ decay matrix elements can explain the simple linear relation between them. References [72, 73] showed that if an operator only probes the short-range physics of low-energy states, the corresponding matrix elements factorize into a universal operator-dependent constant times a state-dependent number common to all short-range operators. A linear relation between the DGT and $0\nu\beta\beta$ decay matrix elements follows. Our correlation depends moderately on the mass region probably because of the approximate cancellation of intermediate- and long-range contributions in the DGT matrix elements. This explanation is consistent with the different pattern of the QRPA results, as QRPA DGT transitions do not show any cancellation between intermediate and long internucleon distances [69], contrary to the shell model.

Another difference between shell model and QRPA DGT matrix elements appears when Eq. (6) is evaluated introducing a complete set of intermediate states. While in the QRPA intermediate 1^+ states up to 15 MeV can be relevant [69], typically canceling low-energy contributions, in the shell model the impact of 1^+ states be-

yond 8 MeV is minor [22]. A possible reason is that shell model calculations, except for ^{48}Ca , miss spin-orbit partners needed to reproduce the GT GR at 10-15 MeV. This difference may be connected to the disagreement between QRPA and shell model results in Fig. 4. On the other hand, the good correlation between shell model DGT and $0\nu\beta\beta$ decay matrix elements suggests that intermediate states may not be decisive, because DGT transitions involve 1^+ states only, while $0\nu\beta\beta$ decay is dominated by intermediate states with other angular momenta [66–68, 71].

The linear correlation between the DGT transition and $0\nu\beta\beta$ decay in Fig. 4 could be used to constrain the value of NMEs from DGT experiments. However measuring the M^{DGT} to the ground state is a formidable challenge. Our calculations predict that this transition accounts for only about 0.03 per mil of the total DGT strength. Clean experiments as well as elaborate analysis are necessary [25].

Corrections to the correlations found in this work may arise from the renormalization of the $0\nu\beta\beta$ or DGT operators due to missing many-body correlations [74–76], two-body currents [77], or an axial tensor polarizability [78]. Nonetheless updated correlations could be obtained adding the new contributions to the matrix elements defined in Eqs. (3) and (6).

Summary. We have performed large-scale shell model calculations that suggest that double charge-exchange reactions can be a very valuable tool to constrain $0\nu\beta\beta$ decay NMEs. Our study indicates that if theoretical calculations reproduce upcoming DGT transition data as they do with GT strength distributions, the experimental energy of the DGT GR will inform on the ^{48}Ca $0\nu\beta\beta$ decay NME value. More generally, we have found a linear correlation between the DGT transition to the final nucleus ground state and the $0\nu\beta\beta$ decay NME. The correlation originates in the dominant short-range character of both transitions. Recent and planned experiments looking for DGT strength distributions will test our theoretical predictions and open the door to constraining $0\nu\beta\beta$ decay NMEs in double charge-exchange experiments.

Acknowledgments. We thank Scott K. Bogner, Yutaka Utsuno, and Motonobu Takaki for very stimulating discussions. This work was supported by JSPS KAKENHI Grant (25870168, 17K05433) and CNS-RIKEN joint project for large-scale nuclear structure calculations. It was also supported by MEXT and JICFuS as a priority issue (Elucidation of the fundamental laws and evolution of the universe, hp170230) to be tackled by using Post K Computer.

* shimizu@cns.s.u-tokyo.ac.jp

† menendez@cns.s.u-tokyo.ac.jp

- [1] A. Gando *et al.* (KamLAND-Zen Collaboration) Phys. Rev. Lett. **117**, 082503 (2016).
- [2] M. Agostini *et al.* (GERDA Collaboration), Nature **544**, 47 (2017).
- [3] J. B. Albert *et al.* (EXO-200 Collaboration), Nature **510**, 229 (2014).
- [4] K. Alfonso *et al.* (CUORE Collaboration), Phys. Rev. Lett. **115**, 102502 (2015).
- [5] F. T. Avignone III, S. R. Elliott, J. Engel, Rev. Mod. Phys. **80**, 481 (2008).
- [6] J. Engel, and J. Menéndez, Rep. Prog. Phys. **80**, 046301 (2017).
- [7] S. J. Freeman, and J. P. Schiffer, J. Phys. G: Nucl. Part. Phys. **29**, 124004 (2012).
- [8] B. P. Kay *et al.*, Phys. Rev. C **87**, 011302(R) (2013).
- [9] J. P. Entwisle *et al.*, Phys. Rev. C **93**, 064312 (2016).
- [10] S. V. Szwece *et al.*, Phys. Rev. C **94**, 054314 (2016).
- [11] B. A. Brown, M. Horoi, and R. A. Sen'kov, Phys. Rev. Lett. **113**, 262501 (2014).
- [12] A. S. Barabash, Nucl. Phys. A **935**, 52 (2015).
- [13] M. Horoi, and A. Neacsu, Phys. Rev. C **93**, 024308 (2016).
- [14] J. Barea, J. Kotila, and F. Iachello, Phys. Rev. C **91**, 034304 (2015).
- [15] J. Suhonen, and O. Civitarese, J. Phys. G: Nucl. Part. Phys. **39**, 085105 (2012).
- [16] V. A. Rodin, A. Faessler, F. Simkovic, and P. Vogel, Nucl. Phys. A **766**, 107 (2006).
- [17] E. Caurier, A. Poves, and A. P. Zuker, Phys. Lett. B **252**, 13 (1990).
- [18] M. Ichimura, H. Sakai, and T. Wakasa, Prog. Part. Nucl. Phys. **56**, 446 (2006).
- [19] D. Frekers, P. Puppe, J. H. Thies, and H. Ejiri, Nucl. Phys. A **916**, 219 (2013).
- [20] K. Yako *et al.*, Phys. Rev. Lett. **103**, 012503 (2009).
- [21] J. Suhonen, and O. Civitarese, Phys. Lett. B **725**, 153 (2013).
- [22] E. Caurier, F. Nowacki, and A. Poves, Phys. Lett. B **711**, 62 (2012).
- [23] T. R. Rodríguez, G. Martínez-Pinedo, Prog. Part. Nucl. Phys. **66**, 436 (2011).
- [24] T. R. Rodríguez, G. Martínez-Pinedo, Phys. Lett. B **719**, 174 (2013).
- [25] F. Cappuzzello, M. Cavallaro, C. Agodi, M. Bondi, D. Carbone, A. Cunsolo and A. Foti, Eur. Phys. J. A **51**, 145 (2015).
- [26] S. J. Greene *et al.*, Phys. Rev. C **25**, 927 (1982).
- [27] P. Vogel, M. Ericson, and J. D. Vergados, Phys. Lett. B **212**, 259 (1988).
- [28] N. Auerbach, L. Zamick and D. C. Zheng, Annals of Physics **192**, 77 (1989).
- [29] D. C. Zheng, L. Zamick and N. Auerbach, Phys. Rev. C **40** 936 (1989).
- [30] D. C. Zheng, L. Zamick, and N. Auerbach, Annals of Physics **197**, 343 (1990).
- [31] K. Muto, Phys. Lett. B **277**, 13 (1992).
- [32] H. Sagawa and T. Uesaka, Phys. Rev. C **94**, 064325 (2016).
- [33] M. Takaki *et al.*, JPS Conf. Proc. **6**, 020038 (2015).
- [34] K. Takahisa *et al.*, arXiv:1703.08264.
- [35] M. Takaki *et al.*, CNS Annual Report **94**, 9 (2014).
- [36] T. Uesaka *et al.*, RIKEN RIBF NP-PAC, NP1512-RIBF141 (2015).
- [37] R. Arnold *et al.*, Phys. Rev. D **93**, 112008 (2016).

- [38] T. Iida et al., J. Phys.: Conf. Ser. **718**, 062026 (2016).
- [39] Yu. G. Zdesenko *et al.*, Astropart. Phys. **23**, 249 (2005).
- [40] L. S. Song, J. M. Yao, P. Ring, and J. Meng, Phys. Rev. C **95**, 024305 (2017).
- [41] Y. Iwata, N. Shimizu, T. Otsuka, Y. Utsuno, J. Menéndez, M. Honma, and T. Abe, Phys. Rev. Lett. **116**, 112502 (2016).
- [42] A. A. Kwiatkowski *et al.*, Phys. Rev. C **89**, 045502 (2014).
- [43] N. López Vaquero, T. R. Rodríguez, and J. L. Egido, Phys. Rev. Lett. **111**, 142501 (2013).
- [44] R. A. Sen'kov and M. Horoi, Phys. Rev. C **88**, 064312 (2013).
- [45] F. Šimkovic, V. Rodin, A. Faessler, and P. Vogel, Phys. Rev. C **87**, 045501 (2013).
- [46] J. Menéndez, A. Poves, E. Caurier, and F. Nowacki, Nucl. Phys. A **818**, 139 (2009).
- [47] R. R. Whitehead, A. Watt and D. Kelvin, Phys. Lett. B **89**, 313 (1980).
- [48] E. Caurier, G. Martínez-Pinedo, F. Nowacki, A. Poves and A. P. Zuker, Rev. Mod. Phys. **77** 427 (2005).
- [49] N. Shimizu, arXiv:1310.5431 [nucl-th].
- [50] M. Honma, T. Otsuka, and T. Mizusaki, RIKEN Accelerator. Progress Report **41**, 32 (2008).
- [51] A. Poves, J. Sanchez-Solano, E. Caurier, and F. Nowacki, Nucl. Phys. A **694**, 157 (2001).
- [52] A. Poves, G. Martínez-Pinedo, Phys. Lett. B **430**, 203 (1998).
- [53] M. Dufour and A. P. Zuker, Phys. Rev. C **54**, 1641 (1996).
- [54] E. Caurier, J. Menéndez, F. Nowacki, and A. Poves, Phys. Rev. Lett. **100**, 052503 (2008).
- [55] J. Barea, and F. Iachello, Phys. Rev. C **79**, 044301 (2009).
- [56] B. A. Brown, D. L. Fang, and M. Horoi, Phys. Rev. C **92**, 041301(R) (2015).
- [57] P. Vogel and M. R. Zirnbauer, Phys. Rev. Lett. **57**, 3148 (1986).
- [58] J. Engel, P. Vogel and M. R. Zirnbauer, Phys. Rev. C **37**, 731 (1988).
- [59] N. Hinohara, and J. Engel, Phys. Rev. C **90**, 014301(R) (2014).
- [60] J. Menéndez, N. Hinohara, J. Engel, G. Martínez-Pinedo, and T. R. Rodríguez, Phys. Rev. C **93**, 014305 (2016).
- [61] E. Caurier, A. Poves, and A. P. Zuker, Phys. Rev. Lett. **74**, 1517 (1995).
- [62] Y. Iwata, N. Shimizu, T. Otsuka, Y. Utsuno, M. Honma, and T. Abe, JPS Conf. Proc. **6**, 030057 (2015).
- [63] M. Honma, T. Otsuka, T. Mizusaki, and M. Hjorth-Jensen, Phys. Rev. C **80**, 064323 (2009).
- [64] B. A. Brown, private communication.
- [65] C. Qi, and Z. X. Xu, Phys. Rev. C **86**, 044323 (2012).
- [66] R. A. Sen'kov, M. Horoi, and B. A. Brown, Phys. Rev. C **89**, 054304 (2014).
- [67] A. Neacsu, and M. Horoi, Phys. Rev. C **91**, 024309 (2015).
- [68] R. A. Sen'kov, and M. Horoi, Phys. Rev. C **93**, 044334 (2016).
- [69] F. Šimkovic, R. Hodák, A. Faessler, and P. Vogel, Phys. Rev. C **83**, 015502 (2011).
- [70] J. Menéndez, T. R. Rodríguez, G. Martínez-Pinedo, and A. Poves, Phys. Rev. C **90**, 024311 (2014).
- [71] F. Šimkovic, A. Faessler, V. Rodin, P. Vogel, and J. Engel, Phys. Rev. C **77**, 045503 (2008).
- [72] E. R. Anderson, S. K. Bogner, R. J. Furnstahl, and R. J. Perry, Phys. Rev. C **82**, 054001 (2010).
- [73] S. K. Bogner, and D. Roscher, Phys. Rev. C **86**, 064304 (2012).
- [74] G. F. Bertsch, and I. Hamamoto, Phys. Rev. C **26**, 1323 (1982).
- [75] A. Arima, K. Shimizu, W. Bentz, and H. Hyuga, Adv. Nucl. Phys. **18**, 1 (1987).
- [76] I. S. Towner, Phys. Rep. **155**, 263 (1997).
- [77] J. Menéndez, D. Gazit, and A. Schwenk, Phys. Rev. Lett. **107**, 062501 (2011).
- [78] P. E. Shanahan, B. C. Tiburzi, M. L. Wagman, F. Winter, E. Chang, Z. Davoudi, W. Detmold, K. Orginos, and M. J. Savage, Phys. Rev. Lett. **119**, 062003 (2017).